Journal of Cellular Biochemistry 101:399–410 (2007)

Temporal Evolution of Gene Expression in Rat Carotid Artery Following Balloon Angioplasty

Jian-ming Li,[1]* Xueqing Zhang,[3] Peter R. Nelson,[5] Paul R. Odgren,[4] Janice D. Nelson,[5] Calin Vasiliu,[2] Jane Park,[2] Marvin Morris,[2] Jane Lian,[4] Bruce S. Cutler,[1] and Peter E. Newburger[3]

[1]Department of Surgery, Division of Vascular Surgery, University of Massachusetts Medical School, 55 Lake Avenue North, Worcester, Massachusetts
[2]Department of Surgery, Division of General Surgery, University of Massachusetts Medical School, 55 Lake Avenue North, Worcester, Massachusetts
[3]Department of Pediatrics, Division of Hematology-Oncology, University of Massachusetts Medical School, 55 Lake Avenue North, Worcester, Massachusetts
[4]Department of Cell Biology, University of Massachusetts Medical School, 55 Lake Avenue North, Worcester, Massachusetts
[5]The Division of Vascular Surgery and Endovascular Therapy, University of Florida College of Medicine, Gainsville, Florida

Abstract The success of vascular intervention including angioplasty, stenting, and arterial bypass remains limited by negative remodeling resulted in lumen restenosis. This study was to characterize the global transcription profile reflecting concurrent events along arterial remodeling and neointima formation in a rat carotid artery balloon-injury model. Expression profiling of injured and control common carotid arteries on days 4, 7, 14 post-injury that mark the major pathohistological progression stages of neointimal formation were recorded on high-density oligonucleotide arrays. A subset of genes from microarray-based data was further studied using quantitative real time RT-PCR and in situ hybridization with sequential arterial samples from days 1 to 28 post-injury. The gene-encoded proteins were validated with Western blot. Besides temporal induction of a large cluster of genes over-represented by cell proliferation and macromolecule metabolism gene ontology categories, a fast-evolving inflammation could be demonstrated by the induction of Tgfb and other anti-inflammatory genes (e.g., C1qtnf3 (C1q and tumor necrosis factor related protein 3 (predicted))) and a shift from type 1 to 2 helper T cell response. The most significant signature of the induced neointimal profile is enrichment of genes functionally related to angiogenesis and extracellular matrix (ECM) remodeling (e.g., Spp1 (secreted phosphoprotein 1), CD44 (CD44 antigen), and Cxcl12 (chemokine (C-X-C motif) ligand 12 (stromal cell-derived factor 1)). Some of the genes represent stress-responsive mesenchymal stromal cell cytokines. This study highlighted mesenchymal stromal cell cytokines-driven inflammatory extracellular matrix remodeling, as target processes for potential clinical therapeutic intervention. J. Cell. Biochem. 101: 399–410, 2007.

Key words: angioplasty; restenosis; remodeling; gene expression; inflammation; leukocytes; lymphocytes; SMC

Percutaneous angioplasty with intracoronary stenting, although well established as the treatment of choice for coronary stenosis, still carries the risk of complications, particularly in-stent restenosis and thrombosis [Muni and Gross, 2004; van der Hoeven et al., 2005]. These

This article contains supplementary material, which may be viewed at the Journal of Cellular Biochemistry website at http://www.interscience.wiley.com/jpages/0730-2312/suppmat/index.html.

Jian-ming Li and Xueqing Zhang contributed equally to this work.

Grant sponsor: The Ellinwood Endowment (to B.S.C.); Grant sponsor: Bugher Foundation (to J.M.L.); Grant sponsor: NIH (to P.E.N.); Grant number: R01DK54369; Grant sponsor: NIDCR (to P.R.O.); Grant number: R01DE07444.

*Correspondence to: Jian-ming Li, MD, Department of Surgery, Division of Vascular Surgery, University of Massachusetts Medical School, 55 Lake Avenue North, Worcester, MA 01655. E-mail: jianming.li@umassmed.edu

Received 4 August 2006; Accepted 4 October 2006
DOI 10.1002/jcb.21190

risks are higher in patients requiring multiple stents or with an underlying disorder such as diabetes [Dibra et al., 2005; Finn et al., 2005]. In addition to the well-known influence of arterial trauma and intraluminal thrombosis on vascular smooth muscle cell (VSMC) proliferation, local inflammation also plays a critical role in neointima formation and restenosis [Wainwright et al., 2001; Farb et al., 2002]. Neointima formation, which corresponds to the fibroproliferative stage of wound healing, consists of multiple processes, including not only VSMC proliferation, but also angiogenesis, vascular remodeling and extracellular matrix (ECM) deposition [Farb et al., 2004].

Numerous studies have examined the processes leading to neointimal formation under many different experimental and clinical settings. High-throughput microarray analysis of gene expression provides a way to understand the complexity of the underlying molecular pathology of cardiovascular disease and to identify suitable target genes for therapy [Levy and Muldowney, 2002]. A number of microarray studies have examined major cardiovascular diseases including microscopic specimens of human stent-induced neointima samples [Zohlnhofer et al., 2001a,b; Kotani et al., 2003]. Considerable knowledge about restenosis and neointima formation has come from animal model studies, including both balloon angioplasty and stenting models [De Meyer and Bult, 1997; Welt and Rogers, 2002]. However, the detailed spatial and temporal gene differential expressions upon vessel injury and their pathways of stimulating intimal hyperplasia formation have not been laid out yet. In general, stenting induces more prolonged inflammation and macrophage recruitment within the neointima, whereas balloon angioplasty alone leads to a more rapidly-evolving process with more neutrophil invasion, endothelial regeneration, and more severe constrictive neointimal remodeling [Nakatani et al., 2003; Kipshidze et al., 2004].

Here we examined the temporal patterns of gene expression in a balloon-injured rat carotid artery model [Clowes et al., 1983]. Using high density oligonucleotide microarray analysis in parallel with real-time PCR, in situ hybridization, Western blot and histology, we have compared transcript profile levels in injured artery tissue to that in sham-operated and normal controls. In addition to the expected induction of expression in genes involved in VSMC migration and proliferation, we found striking, transient up-regulation of genes associated with growth factors, cytokines, and mesenchymal (e.g., stromal) cell proliferation and migration. Later and more long-lasting changes occurred in genes encoding extracellular matrix (ECM) components and muscle contractile proteins. This study highlighted the importance of temporal inflammatory mediators, mesenchymal cells, and ECM components in the molecular pathophysiology of neointimal hyperplasia and restenosis following angioplasty and suggests multiple potential targets for future intervention by gene suppression.

MATERIALS AND METHODS

Rat Carotid Artery Balloon Injury and Sample Collection

The procedures on animals were in accordance with the University of Massachusetts Medical School guidelines. General anesthesia was induced in a 5% isofluorane box, and maintained with 1%–2% isoflurane inhalation through a cone-mask. Analgesia with buprenorphine 0.04 mg/kg was given subcutaneously pre-operatively and every 8 h for 48 h post-operatively. The left common carotid artery of male rats (white Sprague–Dawley, body weight 540 ± 50 g, total 210) was injured using a 2F arterial embolectomy catheter (Fogarty®, Edwards Lifesciences™) introduced through the external carotid artery with inflation and deflation three times to expand the artery and denude endothelium. The contralateral common carotid artery was subjected to a sham procedure as self-control. For RNA isolation, bilateral carotid arteries were retrieved at days 1, 2, 4, 7, 14, and 28, and placed immediately in RNA*later*® (Ambion) on ice. The adventitia of both arteries and the endothelium of the right (uninjured) artery were quickly removed and remaining tissue were snap-frozen and then stored at -80°C for later processing. Uninjured bilateral carotid arteries from healthy rats were also harvested for RNA isolation as normal controls. For Western blot analysis, both post balloon-injured (days 1, 4, 7, and 14) and bilateral normal control carotid artery specimens were harvested, snap-frozen after removal of adventitia and endothelium, and stored at -80°C for later protein extraction. For

histological examination and in situ hybridization, the artery samples were harvested after perfusion fixation with 4% paraformaldehyde at 110–120 mmHg pressure for 30 min. Samples were later processed for paraffin embedding and microtome section after 48 h fixation in 4% paraformaldehyde.

Oligonucleotide Array Transcription Profiling

This study utilized the high-density oligonucleotide GeneChip, Rat Expression Array 230A (Affymetrix), which contains 15,000 sequences representing 10,100 gene loci. All procedures followed the manufacturer's protocols (www. affymetrix.com/support/technical/manual/expression_manual.affx). Time course specimens were collected from normal uninjured and balloon-injured carotid arteries at days 4, 7, and 14 post balloon-injury. Briefly, 3–6 carotid artery specimens were pooled for isolation of total RNA by TRIzol Reagent (Invitrogen). RNA was further purified by elution from RNeasy Mini spin columns (QIAGEN) following DNase digestion. The quality of total RNA preparations was monitored by agarose gel electrophoresis prior to the reverse transcription of cDNA and biotin labeling of cRNA for oligonucleotide array hybridization. Hybridization images were generated by GeneChip Operating System (Affymetrix).

Statistics and Bioinformatic Analysis of Gene Expression Profile

Statistical and gene ontology analyses and visualizations employed standard functions of R language (http://www.R-project.org), R add-on packages from BioConductor project [Gentleman et al., 2004], and DNA-Chip Analyzer (dChip) software [Li and Wong, 2001]. Gene expression values were normalized by either quantile method (BioConductor) or invariant set method (dChip. Non-expressed probe sets were filtered out by both a threshold of Affymetrix P (present) call (100%) and of signal value (>median intensity cross all arrays) without passing in any group of samples. The data of remaining probe sets were constructed as an input matrix. The differences between control and experimental groups were tested by local-pooled-error test (LPE) [Jain et al., 2003], and *P*-values were adjusted to control the false discovery rate (FDR). The differences were also quantitatively measured as difference of group means and lower 90% confidence bound of fold change (Fc) by group comparison analysis of dChip. To identify differentially expressed genes from other genes expressed above background, criteria of both adjusted *P*-value and quantitative measures were applied and should be past in at least one time-point. Most significant differentially expressed genes were further sorted by higher Fc criterion.

Principal component analysis (PCA), as developed by Challacombe et al. [2004], and Kluger et al. [2003] was used to analyze the time-related expression patterns associated with neointima formation. Principal components or eigengenes [Alter et al., 2000] were calculated from the correlation matrix of the genes by calling the R function "prcom," with each gene of input matrix (across all samples) previously standardized. The correlations of transcriptional profiles of all input genes to the profile of dominant eigengenes were calculated and visualized by a scatter plot, on which the isolated region with significantly higher density represents a cluster of genes with similar profiles defined by their similar correlations to the eigengenes. These clusters were cut by contour lines of threshold densities to extract the cluster members by their Affymetrix probe set ID. Significant associations of PCA clusters with gene ontology categories of biological process were determined by a hypergeometric test based on up-to-date metadata of gene annotation from BioConductor project.

Real Time Quantitative RT-PCR (RT-PCR)

A two-step quantitative reverse transcription- polymerase chain reaction (RT-PCR) was employed to quantify mRNA expression levels of CD44, osteopontin (Spp1), interleukin 18 (IL18), transforming growth factor beta 2 (Tgfb2), procollagen XII α1 (Col12α1), insulin-like growth factor 2 (Igf2), and C1q and tumor necrosis factor related protein 3 (C1qtnf3). Time course specimens were collected from normal uninjured and balloon-injured carotid arteries at days 2, 4, 7, 14, and 28 post balloon-injury. Total RNA was extracted from two to six pooled rat artery specimens. The first-strand cDNAs were synthesized with an anchored oligo(dT) primer. Real-time PCR was performed on an Applied Biosystems 7300 Real Time PCR System. The relative standard curve derived from serial dilutions of sample first-strand cDNA was used for quantification. Levels of target genes were normalized over

the internal control gene Rps6 (ribosomal protein s6).

Western Blot

For Western blot verification of protein expression specimens were collected from uninjured and balloon-injured carotid arteries at days 1, 4, 7, and 14 post balloon-injury. A sets of two artery samples were pooled and homogenized in Cell Lysis Buffer (Cell Signaling Technology) supplemented with Protease Inhibitor Cocktail (Sigma) using a Polytron PT2100 (Brinkmann) homogenizer. Supernatant protein was quantified by BCA assay (Pierce Biotechnology). Proteins were loaded with equal quantity for both uninjured (control) and injured arteries at each time point. Sample proteins were separated on 10% precast polyacrylamide gels (Bio-Rad) and then electro-transferred to PVDF membranes (Immobilon^{TM}—P, Millipore). The membranes were probed with anti-rat osteopontin (Spp1) (Assay Designs) and anti-rat CD44 (Antigenix America). The signal was detected with Western Lighting Chemiluminescence Reagent Plus (PerkinElmer Life Sciences, MA) and exposed with BioMax XAR film (Kodak).

In Situ Hybridization (ISH)

A previously-reported non-radioactive ISH method [Marks et al., 1999] was used to study serial sections of carotid artery samples that were collected as described above and cut in 5 μm sections. Selected sections of un-injured control and balloon-injured samples at days 1, 2, 4, 7, and 28 post balloon angioplasty were hybridized with a digoxigenin (DIG) labeled riboprobe for Spp1 mRNA prepared as previously described [Odgren et al., 2003]. In brief, after deparaffinization in xylene and hydration through a graded series of ethanol, sections were rinsed in PBS, exposed to 0.2 M HCl to improve sensitivity, permeabilized by exposure to proteinase K (20 μg/ml), and rinsed in 0.2% glycine to quench enzyme digestion, and post-fixed in 4% paraformaldehyde. Sections were then exposed to triethanolamine with acetic anhydride to acetylate positively-charged amino groups and immersed in the prehybridization solution (2 × SSC/50% deionized formamide) to enhance hybridization. Hybridization was performed in the presence of hybridization buffer containing 0.5 ng DIG-UTP-labeled riboprobe/μl overnight at 42°C in a sealed humid chamber. Following hybridization, a series of high stringency washes (SSC of varying strength and 50% formamide with 2 × SSC, and RNase A treatment (20 μg/ml) to remove weakly hybridized and unhybridized probe. The locations of specifically bound DIG-labeled riboprobes were detected by reacting with an anti-DIG antibody coupled to alkaline phosphatase (Boehringer Mannheim). Phosphatase activity was identified histochemically as a red-purple precipitate using 450 μg/ml nitroblue tetrazolium and 175 μg/ml of 5-bromo-4-chloro-3-indolyl phosphate in 100 mM Tris-HCl, pH 9.5, containing 100 mM NaCl and 50 mM $MgCl_2$. Exposure times for development typically range from 50 to 150 min depending upon the sensitivity of probe and the specimen. Color development was stopped at the same time in all samples by rinsing in Tris-HCl buffer. Sections were then covered with a water-based mounting medium (Aqua Perm, Immunon, Pittsburgh, PA), dried and mounted using Permount (Fisher Scientific).

RESULTS

Histology of Neointimal Hyperplasia

Neointima formation progressed after dilatation and endothelial denuding of rat carotid arteries by balloon angioplasty, as shown in Figure 1. The endothelium was depleted following balloon-injury. At day 4 post-injury, the internal elastic lamina was interrupted, the VSMC in the media was severely damaged, a small mural thrombus was present, and inflammatory cells had adhered to the vessel wall and infiltrated into the media (data not shown). At day 7 regional neointima became thicker. Aggressive circumferential neointimal growth was observed at day 14 and 28, but the thickness of neointima did not increase significantly after day 14. Platelets adhered to the luminal surface and inflammatory cells infiltrated into the media from the very beginning and were still seen at day 7 (data not shown). The histological appearance of these arteries is consistent with prior observations in this model system [Clowes et al., 1983] and in our rabbit femoral artery balloon angioplasty model [Li et al., 2004]. There were no visible changes of the arterial wall on the sham control side.

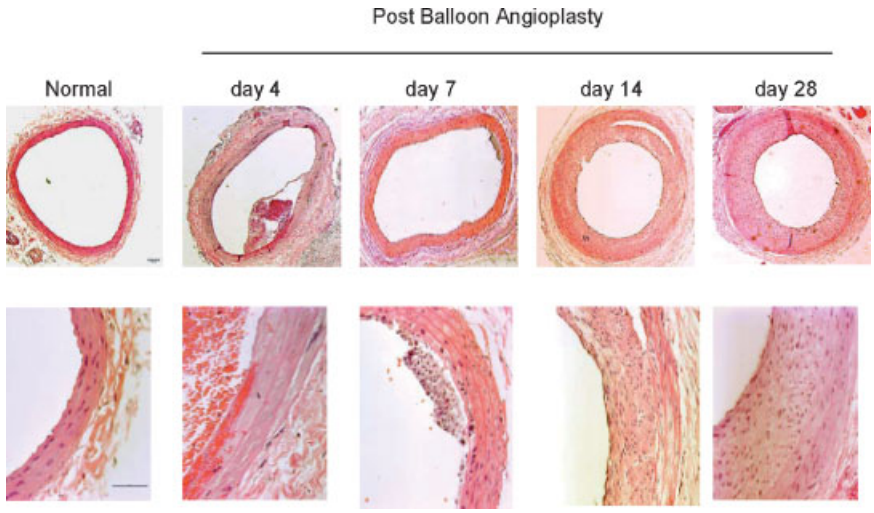

Fig. 1. Microphotographs of representative cross-sections of rat carotid artery after balloon injury. Hematoxylin-eosin stain. Original magnification 4× (top row, bar = 100 μm) and 30× (bottom row, bar = 50 μm).

Temporal Patterns of Gene Expression

RNA samples isolated from balloon-injured, contralateral sham control, and normal control arteries at days 4, 7, and 14 post balloon angioplasty were profiled on RAE230A GeneChips. Many transcripts underwent significant induction or suppression after the balloon injury, and with the most dramatic changes occurring in the first week (Table I and Supplement Table 1 online). At day 4, fewer differentially expressed transcripts were identified in the comparison of injured artery versus sham controls in the same animal, relative to normal controls in untreated rats. This difference may reflect a systemic response to injury that affects the contralateral sham-operated artery.

Measured by a higher threshold (lower bound of 90% confidence interval of fold change >3, and difference of group mean >median signal of all arrays), 101 known genes showed the most significant changes in expression (Fig. 3). Most strikingly, 37 of these genes encode extracellular proteins, including 15 associated with the extracellular matrix. Other over-represented gene function groups included 27 response to stress and immune cell activation genes, 9 cell cycle genes, and 14 cytoskeleton and muscle contraction genes.

PCA was conducted on the entire set of expressed genes to identify the dominant variables, known as eigengenes [Alter et al., 2000; Kluger et al., 2003; Challacombe et al., 2004]. As shown in Figure 2A, two eigengenes captured most of the variance in the data: an early transient up-regulated eigengene 1 (Fig. 2A, left and middle panels) and a more continuously up-regulated eigengene 2 (left

TABLE I. Differentially Expression of Neointima Genes

	Injured versus sham (n ≥ 3)				
Day	$P < 0.01$[a]	Fc[b] > 1.5	$Fc > 3$	Injured versus control (n ≥ 3)	Sham versus control (n ≥ 3)
4	1610	*714*	*71*	2500	23
7	1005	*615*	*48*	1038	61
14	961	*467*	*44*	887	64
Total[c]	2329	*936*	*108*	—	—

[a]Adjusted *P*-value (by FDR).
[b]Lower 90% confidence bound.
[c]Non-redundant, without multiple entries.

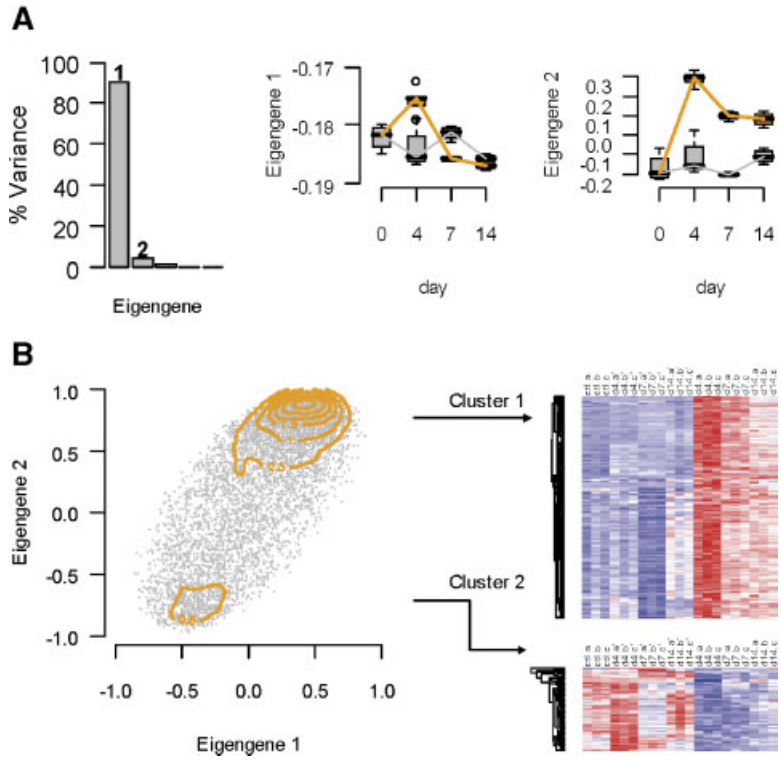

Fig. 2. Principal component analysis of time-related gene expression patterns induced by balloon angioplasty. **Panel A**: Distribution of captured variance across the eigengenes obtained by PCA and plots of temporal profiles corresponding to eigengenes 1 and 2 that recorded most of the variance in the data. **Panel B**: Scatter plot of correlations of the input genes with eigengenes 1 and 2, showing clusters of genes identified by contour lines of density in the correlation plot. The temporal profile of each cluster is presented as a heatmap (for each group n = 3) of cluster members that satisfied both FDR controlled *P*-value (<0.01) and fold change (>1.5) criteria.

and right panels), which also peaked at day 4, but then showed more sustained levels of expression. A scatter plot of correlations of the transcriptional profiles of every input gene to eigengenes 1 and 2 (Fig. 2B) visualized two dense regions that represented two significant gene clusters, indicated by the yellow contour lines. A dense cluster highly correlated with eigengene 2 and also positively to eigengene 1, demonstrated an early induction pattern, as shown by the heatmap for Cluster 1 in Figure 2B. A less dense cluster, negatively correlated to eigengene 1 but uncorrelated to eigengene 2, showed an overall pattern of down-regulation, shown in the heatmap for Cluster 2 in Figure 2B. Cluster 1, defined by a contour line of density 2.0, contained 1361 probe sets, among which 733 (53.9%) were significant in the local-pooled-error (LPE) test and 348 (25.6%) passed a lower 90% confidence bound fold-change (FC) threshold of 1.5 (Supplement Table 1 online). Cluster 2, defined by density threshold of 0.5, contained 413 unique probe sets included 114 LPE significant entries; 71 also passed a lower 90% confidence bound FC threshold of 1.5 (Supplement Table 1 online).

Cluster 1 constitutes the most significant cluster of genes induced by balloon angioplasty. Gene ontogeny groups that are over-represented in this cluster include cellular metabolism and energy generation, intracellular transportation and localization, cell proliferation, apoptosis, cellular morphogenesis, stress responses and immune cell activation (Supplement Table 2a online). For down-regulated Cluster 2, over-represented gene ontogeny groups include myoblast differentiation, muscle development and other differentiation related groups, also genes involved in glucose transport, etc (Supplement Table 2b online). The two complementary clusters temporally match the acute proliferation stage of the fibroproliferative process of wound healing, during which cells in wound granulation tissue dedifferentiate into a proliferative

phenotype; whereas VSMC proliferation is limited to the early time period after arterial injury [Clowes et al., 1983; Farb et al., 2004].

The heatmap presented in Figure 3 shows the expression patterns and gene names for the most highly up- and down-regulated genes, including members of Cluster 1 (red carets [∧]) and Cluster 2 (blue carets [∨]). Some of the most significantly induced genes, including Tgfb1 and those encoding ECM components such as fibronectins and some types of collagens, displayed a pattern of late or sustained induction that differed from the PCA-defined clusters. Very sharp late induction at day 14 occurred in a group of muscle contractile genes (Fig. 3, purple bar; gene names are listed in the right column of the figure).

To validate the different temporal patterns seen in the microarray data, a set of representative genes with different levels and expression patterns were quantified by real time RT-PCR in RNA samples from days 1, 2, 4, 7, 14, 28 post balloon angioplasty (Fig. 4A). Five most significantly induced genes—Cd44/Col12a1 (procollagen, type XII, alpha 1)/Spp1/C1qtnf3/Tgfb1—showed expression patterns matching those observed in oligonucleotide.

Two functionally important genes, Il18 (interleukin [IL]-18) and Igf2 (insulin-like growth factor 2), were also validated quantitatively. Both were measured at low levels on arrays, but showed significant fold changes. The magnitude of their differential expression was confirmed by quantitative RT-PCR (Fig. 3A). A plot of the range of cycle threshold (Ct), corresponding to the range of absolute levels from same amount of inputs (Fig. 3A, lower right panel), also confirmed their low expression levels relative to most of the other genes tested.

Oxidative Stress and Immune Cell Activation

Among the transcripts up-regulated after balloon injury were several genes related to oxidative stress and anti-oxidant defenses. Persistent induced expression of the phagocyte oxidase components Cyba (cytochrome b_{-245}, alpha polypeptide) and Cybb (cytochrome b_{-245}, beta polypeptide) could represent infiltration by neutrophils and macrophages, their activation by local cytokines, or dysfunction of endothelium [Azumi et al., 1999; Guzik et al.,

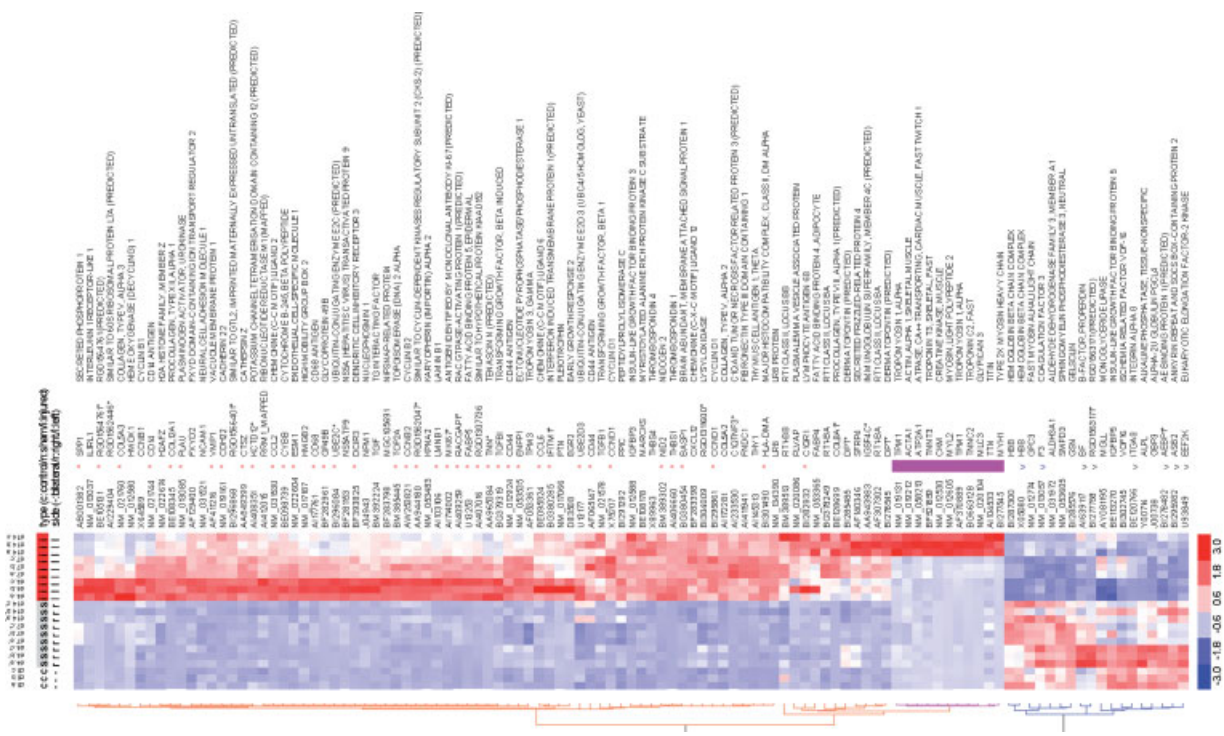

Fig. 3. Heatmap showing the most significantly induced genes with fold changes ≥ 3 (except two entries of CD44, for comparison with Spp1). The red ∧ indicates genes captured in transient cluster 1; the blue ∨, down-regulated genes captured in cluster 2; the purple bar, genes (mainly muscle contraction genes) sharing late induction at day 14.

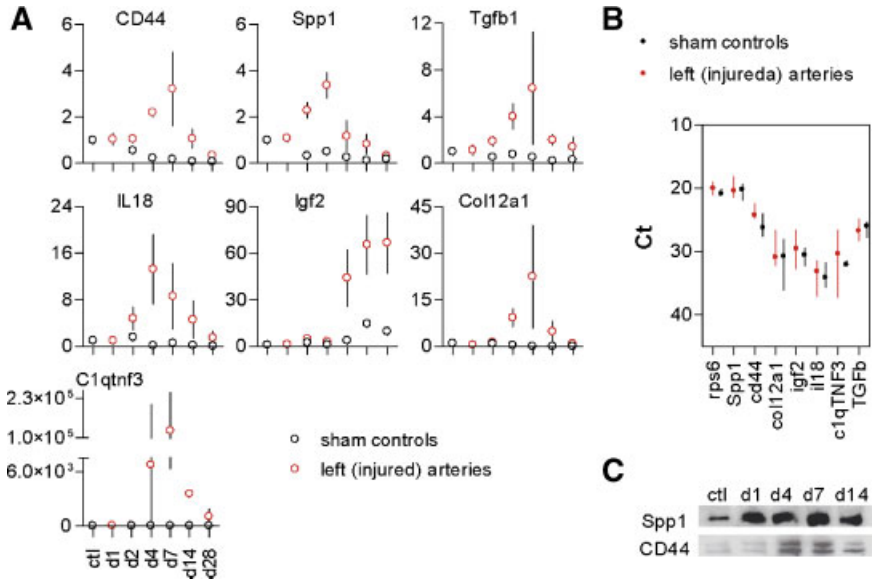

Fig. 4. Quantitative measurements of gene expression at the mRNA and protein levels. **Panel A**: real-time PCR assays of transcript levels for the genes labeled on each graph at the post-injury time points indicated on the lower left margin (''ctl'' = baseline control). Results are presented as mean fold changes (relative to normal control level, after normalization to reference gene Rps6) of three independent experiments. **Panel B**: expression levels of the indicated transcripts (lower margin) presented as range and median of cycle threshold (Ct) of all tested samples of corresponding genes (circles: median of injured artery (solid) and sham controls (open); vertical lines: ranges. **Panel C**: Western blots of Spp1 and CD44 protein levels at the indicated days after balloon angioplasty.

2004]. Additional up-regulated genes representing leukocyte infiltration and activation included Cd14 (CD14, lipopolysaccharide receptor), Fcgr3 (Fc receptor, IgG, low affinity III), Cd68 (CD68 antigen), Cd74 (CD74 antigen; invariant polpypeptide of major histocompatibility class II antigen-associated), Csf1r (macrophage colony-stimulating factor 1 receptor), Mif (macrophage migration inhibitory factor), Hla-dma (major histocompatibility complex, class II, DM alpha), Egr2 (early growth response 2), Il1rl1 (IL-1 receptor-like 1), and Il13ra1 (IL-13 receptor, alpha 1). Persistent induction of Mif and Cd74 indicates a chronic phase of monocyte recruitment and activation [Schober and Weber, 2005]. Expression of negative regulators of T cell activation—including Egr2, Il1rl1, and Il13ra1—suggests local suppression of T cells or a shift from a pro-inflammatory type-1 T helper cell (Th-1) response to a Th-2 response [Hershey, 2003]. Il17r (IL-17 receptor) was also induced (see Supplement Table 1 online), suggesting a role for a newly-described T helper lineage that regulates tissue inflammation [Park et al., 2005]. The induced genes C1qtnf3 and Gp49b (glycoprotein 49b) have also been reported to have anti-inflammatory functions [Weigert et al., 2005; Zhou et al., 2005].

Fibroproliferative Growth Factor Activation

At day 4 after injury there was little or no expression or induction of genes encoding pro-inflammatory cytokines, such as those associated with macrophage activation (e.g., IL-1, IL-6, tumor necrosis factor). However, there was striking induction of genes for growth factors and cytokines associated with the proliferation and migration of mesenchymal stromal cells involved in the local fibroproliferative phase events of wound healing (listed in Fig. 3 and Supplement Table 1 online). Profibrotic growth factors Tgfb1 and Tgfb2 (transforming growth factor beta 1 and 2) that stimulate mesenchymal stromal cells to proliferate and produce ECM in various tissues [Leask and Abraham, 2004], were among the most significantly induced genes (Fig. 3). Similarly-induced and highly expressed was Ctgf (connective tissue growth factor), a downstream effector of Tgfb signaling [Leask and Abraham, 2004]. Actively up-regulated also included the IGF axis genes, Igf1 (Insulin-like growth factor I), Igf2 (Fig. 4A), Igf2r

(Insulin-like growth factor 2 receptor) and Igfbp3 (insulin-like growth factor binding protein 3) (Supplement Table 1 online). Igf1 and Igf2 have been implicated as angiogenic factors involved in wound healing and endothelium recovery [Conti et al., 2004]. Ptn (pleiotrophin), Vegfc (vascular endothelial growth factor C) and Pdgfa (platelet derived growth factor) were other angiogenic growth factor genes induced by injury (Fig. 3 and Supplement Table 1 online).

Cytokine and inflammatory chemokine genes also showed patterns of post-injury induction in the carotid vessel walls, including Mcp1 (monocyte chemotactic protein-1), Ccl2 (chemokine, C-C motif, ligand 2) [Schober et al., 2004], Cxcl12 (chemokine, C-X-C motif, ligand 12, also known as SDF-1, stromal cell-derived factor-1alpha), and Spp1 (secreted phosphoprotein 1, also known as osteopontin). Cxcl12 has been implicated as an angiogenic chemokine for endothelial progenitor cells [Hiasa et al., 2004]. Multifunctional Spp1 is known both as a mediator for skeletal remodeling and as an inflammatory chemoattractant, functionally associated with Cd44 [Denhardt et al., 2001]. Overlapped post balloon-injury expression patterns of Spp1 and Cd44 were demonstrated on RNA levels (Fig. 4A) and Western blots showed parallel changes in the corresponding protein levels (Fig. 4B).

We further investigated the histological localization of Spp1 expression in injured vessels following balloon angioplasty. As shown in Figure 5, in situ hybridization demonstrated Spp1 expression in the media and near adventitia at day 2 after injury (Fig. 5F) before any evidence of neointima formation. At day 4, intense expression was seen in cells on the luminal surface (Fig. 5H), but not in the areas that were positive on day 2. Spp1 expression was weaker and limited to a few cells on the intimal surface by day 7, and was undetectable by 4 weeks. The temporal pattern and localization data suggest that Spp1 functions more as remodeling mediator than a chemoattractant cytokine in this setting.

DISCUSSION

The current study of temporal patterns of gene expression in rat carotid artery was performed at serial time points over 14 days following balloon angioplasty, during a period characterized by neointima formation. We used high density oligonucleotide microarrays for global analysis of gene expression, coupled with real time RT-PCR to confirm and quantitate changes in mRNA levels, plus histology and in situ hybridization to examine tissue morphology and localization of selected transcripts. By comparing gene expression in the injured artery to contralateral sham and normal controls, we identified sets of genes that are significantly up- and down-regulated, in both transient and sustained patterns. In addition to the induction of genes associated with VSMC migration and proliferation, there was a striking, transient increase in the expression of genes encoding growth factors and cytokines implicated in the migration and proliferation of mesenchymal stromal cells. Later in the process, up-regulated genes included several encoding ECM components and muscle contractile proteins.

An early wave of changes in gene expression, represented in two clusters identified by PCA, indicates induction of many genes related to cell proliferation and growth. One possible pathway for the coordinated regulation of these genes involves FK506 binding protein 12-rapamycin associated protein 1 (FRAP1), a protein kinase that synchronizes cell cycle control and protein

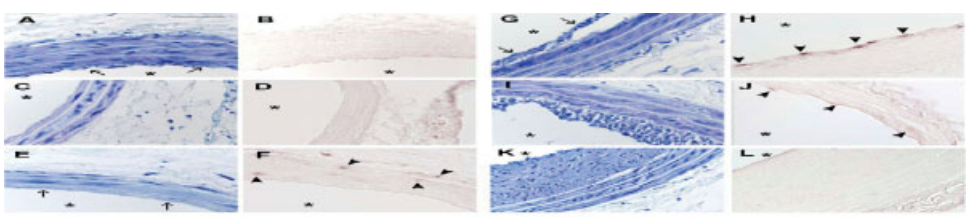

Fig. 5. In situ hybridization of Spp1 transcripts in carotid artery wall after balloon angioplasty. Rat carotid artery cross sections are shown for control (**A**, **B**) and injured arteries at days 1 (**C**, **D**), 2 (**E**, **F**), 4 (**G**, **H**), 7 (**I**, **J**) and 4 weeks (**K**, **L**) following balloon angioplasty. Toluidine blue stain (A, C, E, G, I, K) or in situ hybridization for Spp1 (B, D, F, H, J, L) without counterstain. Bar in panel A = 50 μm. Asterisks denote vessel lumen. Arrows indicate blood-contacting surfaces and arrowheads indicate cells with detectable Spp1 mRNA.

synthesis in neointima formation [Lucchesi, 2004]. Many of its downstream targets take part in the fibroproliferative process. The related gene encoding FK506 binding protein 12 (Fkbp1a), the receptor for rapamycin, has been reported to be up-regulated in human in-stent neointima [Zohlnhofer et al., 2001a]. In the current study, it was significantly induced (fold change <2), and returned to the baseline expression level by day 14. Recent clinical trials of short term rapamycin (sirolimus) eluting stents have shown promise for suppression of neointima growth and restenosis [Dibra et al., 2005; van der Hoeven et al., 2005]. However, other problems related to the stenting, such as delayed wound healing [Kipshidze et al., 2004; Finn et al., 2005; Liuzzo et al., 2005], underscore the need to define more precise pharmacological targets for prevention of stent occlusion.

The inflammatory cytokines IL-17 and IL-18 may also mediate tissue remodeling and angiogenesis. The IL-17 receptor, which was strongly induced in current rat model, mediates tissue inflammation by induction of genes encoding chemokines such as CCL2 [Park et al., 2005]. In addition, IL-17 functions as a stromal cell growth factor that induces potentially angiogenic proliferation of both mesenchymal stem cells and mature stroma cells [Huang et al., 2006]. IL-18 has been shown to mediate tissue remodeling related to intimal thickening and atherosclerotic plaque formation and stability [Mallat et al., 2001; Yamagami et al., 2005; Chandrasekar et al., 2006].

The late up-regulation of muscle contractile genes and sFRP4 (secreted frizzled-related protein 4), an inhibitor of Wnt signaling [He et al., 2005], may mark the end of the fibroproliferative stage of wound healing and neointima growth. For epidermal wounds, contraction is necessary for reepithelialization and full healing. However, after balloon angioplasty the process it may contribute to a constrictive remodeling of neointima [Geary et al., 1998].

Spp1 (also known as osteopontin) and Cd44 may play an important role in stromal tissue remodeling by modulating ECM formation. ECM constitutes more than half of the volume of neointima in injured artery, but the detailed mechanism of its formation has not been defined [Farb et al., 2004]. Spp1 and Cd44 have been implicated as important mediators of neointima hyperplasia and significant markers in atherosclerosis gene profiles; the proteins serve as a conditional ligand-receptor pair and colocalize in vivo [Isoda et al., 2002; Farb et al., 2004; Tabibiazar et al., 2005]. Interaction of Spp1 and Cd44 may represent an important link between inflammation and tissue remodeling, providing a potential mechanism for excessive inflammatory and constrictive ECM remodeling. Our data further suggest that ECM remodeling may be enhanced by other cell migration mechanism and molecules, such as the proteolytic migration molecules Ctsz (cathepsin Z) and Tnn (tenascin N) (Fig. 3). Post-inflammatory ECM remodeling may provide an important biological target for intervention against neointima hyperplasia after angioplasty.

ACKNOWLEDGMENTS

We thank Stephen Baker, MScPH, Senior Biostatistician, and David LaPointe, PhD, Senior Informaticist, University of Massachusetts Medical School for their initial contributions to this project.

REFERENCES

Alter O, Brown PO, Botstein D. 2000. Singular value decomposition for genome-wide expression data processing and modeling. Proc Natl Acad Sci USA 97:10101–10106.

Azumi H, Inoue N, Takeshita S, Rikitake Y, Kawashima S, Hayashi Y, Itoh H, Yokoyama M. 1999. Expression of NADH/NADPH oxidase p22phox in human coronary arteries. Circulation 100:1494–1498.

Challacombe JF, Rechtsteiner A, Gottardo R, Rocha LM, Browne EP, Shenk T, Altherr MR, Brettin TS. 2004. Evaluation of the host transcriptional response to human cytomegalovirus infection. Physiological Genomics 18: 51–62.

Chandrasekar B, Mummidi S, Mahimainathan L, Patel DN, Bailey SR, Imam SZ, Greene WC, Valente AJ. 2006. Interleukin-18-induced human coronary artery smooth muscle cell migration is dependent on NF-{kappa}B- and AP-1-mediated matrix metalloproteinase-9 expression and is inhibited by atorvastatin. J Biol Chem 281: 15099–15109.

Clowes AW, Reidy MA, Clowes MM. 1983. Mechanisms of stenosis after arterial injury. Lab Invest 49:208–215.

Conti E, Carrozza C, Capoluongo E, Volpe M, Crea F, Zuppi C, Andreotti F. 2004. Insulin-like growth factor-1 as a vascular protective factor. Circulation 110:2260–2265.

De Meyer GR, Bult H. 1997. Mechanisms of neointima formation—Lessons from experimental models. Vasc Med 2:179–189.

Denhardt DT, Noda M, O'Regan AW, Pavlin D, Berman JS. 2001. Osteopontin as a means to cope with environmental insults: Regulation of inflammation, tissue remodeling, and cell survival. J Clin Invest 107:1055–1061.

Dibra A, Kastrati A, Mehilli J, Pache J, Schuhlen H, von Beckerath N, Ulm K, Wessely R, Dirschinger J, Schomig A, Investigators I-DS. 2005. Paclitaxel-eluting or sirolimus-eluting stents to prevent restenosis in diabetic patients. N Engl J Med 353:663–670.

Farb A, Weber DK, Kolodgie FD, Burke AP, Virmani R. 2002. Morphological predictors of restenosis after coronary stenting in humans. Circulation 105:2974–2980.

Farb A, Kolodgie FD, Hwang JY, Burke AP, Tefera K, Weber DK, Wight TN, Virmani R. 2004. Extracellular matrix changes in stented human coronary arteries. Circulation 110:940–947.

Finn AV, Kolodgie FD, Harnek J, Guerrero LJ, Acampado E, Tefera K, Skorija K, Weber DK, Gold HK, Virmani R. 2005. Differential response of delayed healing and persistent inflammation at sites of overlapping sirolimus- or paclitaxel-eluting stents. Circulation 112:270–278.

Geary RL, Nikkari ST, Wagner WD, Williams JK, Adams MR, Dean RH. 1998. Wound healing: A paradigm for lumen narrowing after arterial reconstruction. J Vasc Surg 27:96–106.

Gentleman RC, Carey VJ, Bates DM, Bolstad B, Dettling M, Dudoit S, Ellis B, Gautier L, Ge Y, Gentry J, Hornik K, Hothorn T, Huber W, Iacus S, Irizarry R, Leisch F, Li C, Maechler M, Rossini AJ, Sawitzki G, Smith C, Smyth G, Tierney L, Yang JY, Zhang J. 2004. Bioconductor: Open software development for computational biology and bioinformatics. Genome Biol 5:R80.

Guzik TJ, Sadowski J, Kapelak B, Jopek A, Rudzinski P, Pillai R, Korbut R, Channon KM. 2004. Systemic regulation of vascular NAD(P)H oxidase activity and nox isoform expression in human arteries and veins. Arterioscler Thromb Vasc Biol 24:1614–1620.

He B, Lee AY, Dadfarmay S, You L, Xu Z, Reguart N, Mazieres J, Mikami I, McCormick F, Jablons DM. 2005. Secreted frizzled-related protein 4 is silenced by hypermethylation and induces apoptosis in beta-catenin-deficient human mesothelioma cells. Cancer Res 65: 743–748.

Hershey GK. 2003. IL-13 receptors and signaling pathways: An evolving web. J Allergy Clin Immunol 111:677–690.

Hiasa K, Ishibashi M, Ohtani K, Inoue S, Zhao Q, Kitamoto S, Sata M, Ichiki T, Takeshita A, Egashira K. 2004. Gene transfer of stromal cell-derived factor-1alpha enhances ischemic vasculogenesis and angiogenesis via vascular endothelial growth factor/endothelial nitric oxide synthase-related pathway: Next-generation chemokine therapy for therapeutic neovascularization. Circulation 109:2454–2461.

Huang W, La Russa V, Alzoubi A, Schwarzenberger P. 2006. Interleukin-17A: A T-cell-derived growth factor for murine and human mesenchymal stem cells. Stem Cells 24:1512–1518.

Isoda K, Nishikawa K, Kamezawa Y, Yoshida M, Kusuhara M, Moroi M, Tada N, Ohsuzu F. 2002. Osteopontin plays an important role in the development of medial thickening and neointimal formation. Circ Res 91:77–82.

Jain N, Thatte J, Braciale T, Ley K, O'Connell M, Lee JK. 2003. Local-pooled-error test for identifying differentially expressed genes with a small number of replicated microarrays. Bioinformatics 19:1945–1951.

Kipshidze N, Dangas G, Tsapenko M, Moses J, Leon MB, Kutryk M, Serruys P. 2004. Role of the endothelium in modulating neointimal formation: Vasculoprotective approaches to attenuate restenosis after percutaneous coronary interventions. J Am Coll Cardiol 44:733–739.

Kluger Y, Basri R, Chang JT, Gerstein M. 2003. Spectral biclustering of microarray data: Coclustering genes and conditions. Genome Res 13:703–716.

Kotani M, Fukuda N, Ando H, Hu WY, Kunimoto S, Saito S, Kanmatsuse K. 2003. Chimeric DNA-RNA hammerhead ribozyme targeting PDGF A-chain mRNA specifically inhibits neointima formation in rat carotid artery after balloon injury. Cardiovasc Res 57:265–276.

Leask A, Abraham DJ. 2004. TGF-beta signaling and the fibrotic response. FASEB J 18:816–827.

Levy SE, Muldowney JA III. 2002. Microarray analysis of neointima: Flowing toward a clear future. Arterioscler Thromb Vasc Biol 22:1946–1947.

Li C, Wong WH. 2001. Model-based analysis of oligonucleotide arrays: Expression index computation and outlier detection. Proc Natl Acad Sci USA 98:31–36.

Li JM, Singh MJ, Itani M, Vasiliu C, Hendricks G, Baker SP, Hale JE, Rohrer MJ, Cutler BS, Nelson PR. 2004. Recombinant human thrombomodulin inhibits arterial neointimal hyperplasia after balloon injury. J Vasc Surg 39:1074–1083.

Liuzzo JP, Ambrose JA, Coppola JT. 2005. Sirolimus- and taxol-eluting stents differ towards intimal hyperplasia and re-endothelialization. J Invasive Cardiol 17:497–502.

Lucchesi PA. 2004. Rapamycin plays a new role as differentiator of vascular smooth muscle phenotype. focus on "The mTOR/p70 S6K1 pathway regulates vascular smooth muscle differentiation". Am J Physiol—Cell Physiol 286:C480–C481.

Mallat Z, Corbaz A, Scoazec A, Besnard S, Leseche G, Chvatchko Y, Tedgui A. 2001. Expression of interleukin-18 in human atherosclerotic plaques and relation to plaque instability. Circulation 104:1598–1603.

Marks SC Jr, Lundmark C, Wurtz T, Odgren PR, MacKay CA, Mason-Savas A, Popoff SN. 1999. Facial development and type III collagen RNA expression: Concurrent repression in the osteopetrotic (Toothless, tl) rat and rescue after treatment with colony-stimulating factor-1. Dev Dyn 215:117–125.

Muni NI, Gross TP. 2004. Problems with drug-eluting coronary stents–the FDA perspective. N Engl J Med 351: 1593–1595.

Nakatani M, Takeyama Y, Shibata M, Yorozuya M, Suzuki H, Koba S, Katagiri T. 2003. Mechanisms of restenosis after coronary intervention: Difference between plain old balloon angioplasty and stenting. Cardiovascular Pathology 12:40–48.

Odgren PR, Gartland A, MacKay CA. 2003. Production of high-activity digoxigenin-labeled riboprobes for in situ hybridization using the AmpliScribe™ T7 high yield transcription kit. Epi Forum 10:6–7.

Park H, Li Z, Yang XO, Chang SH, Nurieva R, Wang YH, Wang Y, Hood L, Zhu Z, Tian Q, Dong C. 2005. A distinct lineage of CD4 T cells regulates tissue inflammation by producing interleukin 17. Nat Immunol 6:1133–1141.

Schober A, Weber C. 2005. Mechanisms of monocyte recruitment in vascular repair after injury. Antioxidants Redox Signaling 7:1249–1257.

Schober A, Zernecke A, Liehn EA, von Hundelshausen P, Knarren S, Kuziel WA, Weber C. 2004. Crucial role of the

CCL2/CCR2 axis in neointimal hyperplasia after arterial injury in hyperlipidemic mice involves early monocyte recruitment and CCL2 presentation on platelets. Circ Res 95:1125–1133.

Tabibiazar R, Wagner RA, Ashley EA, King JY, Ferrara R, Spin JM, Sanan DA, Narasimhan B, Tibshirani R, Tsao PS, Efron B, Quertermous T. 2005. Signature patterns of gene expression in mouse atherosclerosis and their correlation to human coronary disease. Physiol Genomics 22:213–226.

van der Hoeven BL, Pires NM, Warda HM, Oemrawsingh PV, van Vlijmen BJ, Quax PH, Schalij MJ, van der Wall EE, Jukema JW. 2005. Drug-eluting stents: Results, promises and problems. Int J Cardiol 99: 9–17.

Wainwright CL, Miller AM, Wadsworth RM. 2001. Inflammation as a key event in the development of neointima following vascular balloon injury. Clin Exp Pharmacol Physiol 28:891–895.

Weigert J, Neumeier M, Schaffler A, Fleck M, Scholmerich J, Schutz C, Buechler C. 2005. The adiponectin paralog CORS-26 has anti-inflammatory properties and is produced by human monocytic cells. FEBS Lett 579:5565–5570.

Welt FG, Rogers C. 2002. Inflammation and restenosis in the stent era. Arterioscler Thromb Vasc Biol 22:1769–1776.

Yamagami H, Kitagawa K, Hoshi T, Furukado S, Hougaku H, Nagai Y, Hori M. 2005. Associations of serum IL-18 levels with carotid intima-media thickness. Arterioscler Thromb Vasc Biol 25:1458–1462.

Zhou JS, Friend DS, Lee DM, Li L, Austen KF, Katz HR. 2005. gp49B1 deficiency is associated with increases in cytokine and chemokine production and severity of proliferative synovitis induced by anti-type II collagen mAb. Eur J Immunol 35:1530–1538.

Zohlnhofer D, Klein CA, Richter T, Brandl R, Murr A, Nuhrenberg T, Schomig A, Baeuerle PA, Neumann FJ. 2001a. Gene expression profiling of human stent-induced neointima by cDNA array analysis of microscopic specimens retrieved by helix cutter atherectomy: Detection of FK506-binding protein 12 upregulation. Circulation 103:1396–1402.

Zohlnhofer D, Richter T, Neumann F, Nuhrenberg T, Wessely R, Brandl R, Murr A, Klein CA, Baeuerle PA. 2001b. Transcriptome analysis reveals a role of interferon-gamma in human neointima formation. Mol Cell 7:1059–1069.